RESEARCH ARTICLE SUMMARY

NEUROSCIENCE

# Regulation of sleep homeostasis mediator adenosine by basal forebrain glutamatergic neurons

Wanling Peng*, Zhaofa Wu*, Kun Song*, Siyu Zhang, Yulong Li, Min Xu†

**INTRODUCTION:** Sleep homeostasis, the balance between the duration of sleep and wakefulness, is a fundamental feature of the sleep-wake cycle. During wakefulness, sleep-promoting somnogenic factors accumulate and cause an increase in sleep pressure or our need for sleep. Decades of research have identified many genes, molecules, and biochemical processes involved in the regulation of sleep homeostasis. Among various processes implicated in sleep homeostasis, adenosine—a critical component of the cell metabolic pathway—is a prominent physiological mediator of sleep homeostasis. Adenosine released in the basal forebrain (BF), a brain region that plays a critical role in regulating the sleep-wake cycle, can suppress neural activity mediated by the A1 receptor and increase sleep pressure. In addition, the sleep-wake cycle is controlled by different patterns of neural activity in the brain, but how this neural activity contributes to sleep homeostasis remains mostly unclear. In this study, we examine the neural control of sleep homeostasis by investigating in detail the mechanisms underlying adenosine increase in the BF.

**RATIONALE:** Because the traditional microdialysis measurement of adenosine concentration has a poor temporal resolution, we first designed a genetically encoded G protein–coupled receptor (GPCR)–activation-based (GRAB) sensor for adenosine ($GRAB_{Ado}$), in which the amount of extracellular adenosine is indicated by the intensity of fluorescence produced by green fluorescent protein (GFP) (see the figure, panel A). Using the $GRAB_{Ado}$, we first measured the dynamics of extracellular adenosine concentrations during the sleep-wake cycle in the mouse BF. We then used a simultaneous optical recording of the $Ca^{2+}$ activity in different BF neurons and the change in adenosine concentrations to examine the correlation between adenosine increase and neural activity. We further studied the ability of different BF neurons in controlling the adenosine release using optogenetic activation. Finally, we used cell type–specific lesion to confirm the contribution of BF neurons in controlling the increase in adenosine concentrations and examine its contribution to the sleep homeostasis regulation.

**RESULTS:** We found that the amount of extracellular adenosine was high during wakefulness and low during non–rapid eye movement (NREM) sleep. Benefiting from the high temporal resolution of the $GRAB_{Ado}$, we also found a prominent increase in adenosine during REM sleep and revealed rapid changes in adenosine concentrations during brain state transitions. Simultaneous fiber photometry recording of the $Ca^{2+}$ activity in different BF neurons and the change in extracellular adenosine concentrations showed that both cholinergic neurons and glutamatergic neurons had highly correlated activity with changes in the adenosine concentration (see the figure, panel A). In examining the time course of the two signals, we found that neural activity always preceded changes in adenosine dynamics by tens of seconds. When we measured the evoked adenosine release by optogenetic activation of these two types of neurons using their physiological firing frequencies, we found that the activation of BF cholinergic neurons only produced a moderate increase in extracellular adenosine; by contrast, the activation of BF glutamatergic neurons caused a large and robust increase (see the figure, panel B). Finally, we selectively ablated BF glutamatergic neurons and found a significantly reduced increase in the amounts of extracellular adenosine. Also, mice with a selective lesion of BF glutamatergic neurons showed impaired sleep homeostasis regulation, with significantly increased wakefulness during the active period (see the figure, panel C).

**CONCLUSION:** Here, we report the design and characterization of a genetically encoded adenosine sensor with high sensitivity and specificity, and high temporal resolution; using the sensor, in combination with fiber photometry recording, optogenetic activation, and cell type–specific lesion, we demonstrate a neural activity–dependent rapid dynamics of the extracellular adenosine concentration during the sleep-wake cycle in the mouse BF and uncover a critical role of the BF glutamatergic neurons in controlling adenosine dynamics and sleep homeostasis. These findings suggest that cell type–specific neural activity during wakefulness can contribute to the increase in sleep pressure by stimulating the release of somnogenic factors. ■

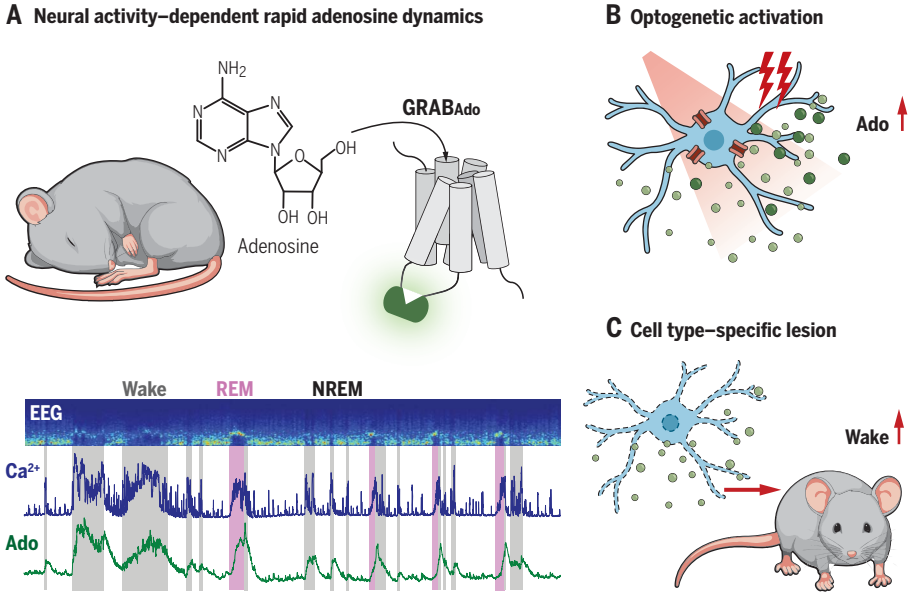


**Neural control of rapid adenosine dynamics and sleep homeostasis.** (**A**) Simultaneous optical recording of the $Ca^{2+}$ activity and adenosine concentration using GCaMP and $GRAB_{Ado}$ reveals neural activity–dependent rapid adenosine dynamics in the mouse basal forebrain (BF) during the sleep-wake cycle. (**B**) Optogenetic activation of BF glutamatergic neurons evokes a robust increase of extracellular adenosine. (**C**) Cell type–specific lesion of BF glutamatergic neurons significantly increases wakefulness.

The list of author affiliations is available in the full article online.
*These authors contributed equally to this work.
†Corresponding author. Email: mxu@ion.ac.cn
Cite this article as W. Peng *et al.*, *Science* **369**, eabb0556 (2020). DOI: 10.1126/science.abb0556

READ THE FULL ARTICLE AT
https://doi.org/10.1126/science.abb0556

RESEARCH ARTICLE

NEUROSCIENCE

# Regulation of sleep homeostasis mediator adenosine by basal forebrain glutamatergic neurons

Wanling Peng[1,2]*, Zhaofa Wu[3,4]*, Kun Song[1,2]*, Siyu Zhang[5,6], Yulong Li[3,4,7], Min Xu[1,6]†

Sleep and wakefulness are homeostatically regulated by a variety of factors, including adenosine. However, how neural activity underlying the sleep-wake cycle controls adenosine release in the brain remains unclear. Using a newly developed genetically encoded adenosine sensor, we found an activity-dependent rapid increase in the concentration of extracellular adenosine in mouse basal forebrain (BF), a critical region controlling sleep and wakefulness. Although the activity of both BF cholinergic and glutamatergic neurons correlated with changes in the concentration of adenosine, optogenetic activation of these neurons at physiological firing frequencies showed that glutamatergic neurons contributed much more to the adenosine increase. Mice with selective ablation of BF glutamatergic neurons exhibited a reduced adenosine increase and impaired sleep homeostasis regulation. Thus, cell type–specific neural activity in the BF dynamically controls sleep homeostasis.

Homeostatic regulation is a fundamental phenomenon of the sleep-wake cycle, and sleep-promoting somnogenic factors accumulate during wakefulness, thereby inducing sleep (*1*, *2*). Several extracellular or cytoplasmic factors and associated biochemical processes that contribute to this phenomenon have been identified (*3*–*5*). In addition, different patterns of neural activity in the brain control the sleep-wake cycle, but how this neural activity contributes to sleep homeostasis remains largely unknown (*6*). Among various processes implicated in controlling sleep homeostasis (*3*, *7*, *8*), the release of adenosine in the basal forebrain (BF) is a prominent physiological mediator of sleep homeostasis (*9*–*12*). In this study, we used a genetically encoded adenosine sensor to examine in detail the mechanisms underlying the increase in adenosine concentration in the BF, a brain region that plays a critical role in regulating the sleep-wake cycle (*13*, *14*).

### Development and characterization of a genetically encoded adenosine sensor

To record the dynamics of extracellular adenosine level in the BF during the sleep-wake cycle with high temporal resolution and high specificity and sensitivity, we designed a genetically encoded G protein–coupled receptor (GPCR)–activation–based (GRAB) sensor for adenosine ($GRAB_{Ado}$), in which the amount of extracellular adenosine is indicated by the intensity of fluorescence produced by green fluorescent protein (GFP) (Fig. 1A).

The sensor was developed by using an established GRAB sensor development pipeline (*15*–*20*): We first screened candidate sensor scaffolds by inserting a conformational-sensitive circularly permuted enhanced GFP (cpEGFP) into different adenosine receptors using linker peptides (fig. S1A); we then selected an $A_{2A}$ receptor ($A_{2A}R$)–based chimera ($GRAB_{Ado0.1}$) for further optimization because of its good membrane trafficking and high fluorescence response upon adenosine application (fig. S1B); we next systematically optimized the length and amino acid composition of the linkers between the $A_{2A}R$ and the cpEGFP and identified a sensor with the largest fluorescence response (fig. S1, C and D), which we named $GRAB_{Ado1.0}$ (hereafter referred to as Ado1.0).

In human embryonic kidney 293T (HEK293T) cells, Ado1.0 showed good membrane trafficking and produced a 120% peak response (change in fluorescence intensity, $\Delta F/F_0$) to the application of a saturated concentration of adenosine (100 μM) (Fig. 1B); by contrast, a non–ligand-binding mutant form of the sensor [F168A (*21*); $GRAB_{Ado1.0mut}$, or Ado1.0mut for short] showed no detectable response (Fig. 1B and fig. S2E). Ado1.0 had rapid response kinetics, with a rise time constant ($\tau_{on}$) of 68 ± 13 ms (Fig. 1C). In neurons, Ado1.0 was widely distributed throughout the membrane, including the soma, axons, and dendrites (Fig. 1D and fig. S2A), and responded to adenosine application in a dose-dependent manner (Fig. 1E and fig. S2C), with a median effective concentration ($EC_{50}$) of ~60 nM (Fig. 1F). Ado1.0 responded to adenosine with high selectivity, because it showed an undetectable or much weaker response to several structurally similar derivatives of adenosine, such as adenosine 5′-diphosphate (ADP), adenosine 5′-triphosphate (ATP), inosine, and adenine (Fig. 1F and fig. S2B). In addition, adenosine-induced fluorescence response can be blocked by the $A_{2A}R$ antagonist SCH-58261 (fig. S2, B to D).

Next, we examined whether Ado1.0 expression affects cellular physiology. Using a luciferase complementation assay, we found that Ado1.0 had almost no downstream $G_s$ coupling, in contrast to the robust coupling produced by cells expressing $A_{2A}Rs$ (Fig. 1H, middle, and fig. S1E, middle). Similarly, we found no detectable downstream cyclic adenosine 3′,5′-monophosphate (cAMP) activation induced by the $A_{2A}R$ agonist HENECA in Ado1.0 (Fig. 1H, right, and fig. S1E, right). Consistent with the minimum activation of intracellular signaling pathways, Ado1.0 showed no detectable internalization, as we observed no significant decrease of fluorescence in Ado1.0-expressing cells when applying a high concentration of adenosine (10 μM) for 2 hours (Fig. 1G and fig. S2D). Finally, there was no difference in either field stimulation–evoked $Ca^{2+}$ signaling (Fig. 1I and fig. S3) or $K^+$-evoked glutamate release (fig. S3) between Ado1.0-expressing neurons and nontransfected neurons, suggesting that expression of Ado1.0 did not measurably alter $Ca^{2+}$ signaling or neurotransmitter release.

Together, these results show that Ado1.0 can detect rapid dynamics of extracellular adenosine levels with high sensitivity and specificity; at the same time, its expression has no detectable effect on cell physiology.

### Dynamics of extracellular adenosine in the sleep-wake cycle

We next examined the dynamics of extracellular adenosine concentration in the BF during the sleep-wake cycle using the $GRAB_{Ado}$ sensor. We injected an adeno-associated virus (AAV) expressing $GRAB_{Ado}$ into the BF and measured the fluorescence signal using fiber photometry through an implanted optical fiber (Fig. 2A and fig. S4); as an internal control (e.g., for correcting movement artifacts), we coexpressed a red fluorescence protein mScarlet, which is insensitive to changes in adenosine concentration. The adenosine signal was then extracted from the measured fluorescence signals using a blind source separation method (*22*).

We observed significantly higher amounts of extracellular adenosine when the mice were awake, as compared with that during non–rapid eye movement (NREM) sleep (Fig. 2B, C, and E; $P = 3.6 \times 10^{-6}$), consistent with previous microdialysis measurements (*9*, *10*). Such a difference was not observed in mice expressing a

[1]Institute of Neuroscience, State Key Laboratory of Neuroscience, Center for Excellence in Brain Science and Intelligence Technology, Chinese Academy of Sciences, Shanghai 200031, China. [2]University of Chinese Academy of Sciences, Beijing 100049, China. [3]State Key Laboratory of Membrane Biology, Peking University School of Life Sciences, Beijing 100871, China. [4]PKU-IDG–McGovern Institute for Brain Research, Beijing 100871, China. [5]Collaborative Innovation Center for Brain Science, Department of Anatomy and Physiology, Shanghai Jiao Tong University School of Medicine, Shanghai 200025, China. [6]Shanghai Center for Brain Science and Brain-Inspired Intelligence Technology, Shanghai 201210, China. [7]Peking-Tsinghua Center for Life Sciences, Academy for Advanced Interdisciplinary Studies, Peking University, Beijing 100871, China.
*These authors contributed equally to this work.
†Corresponding author. Email: mxu@ion.ac.cn

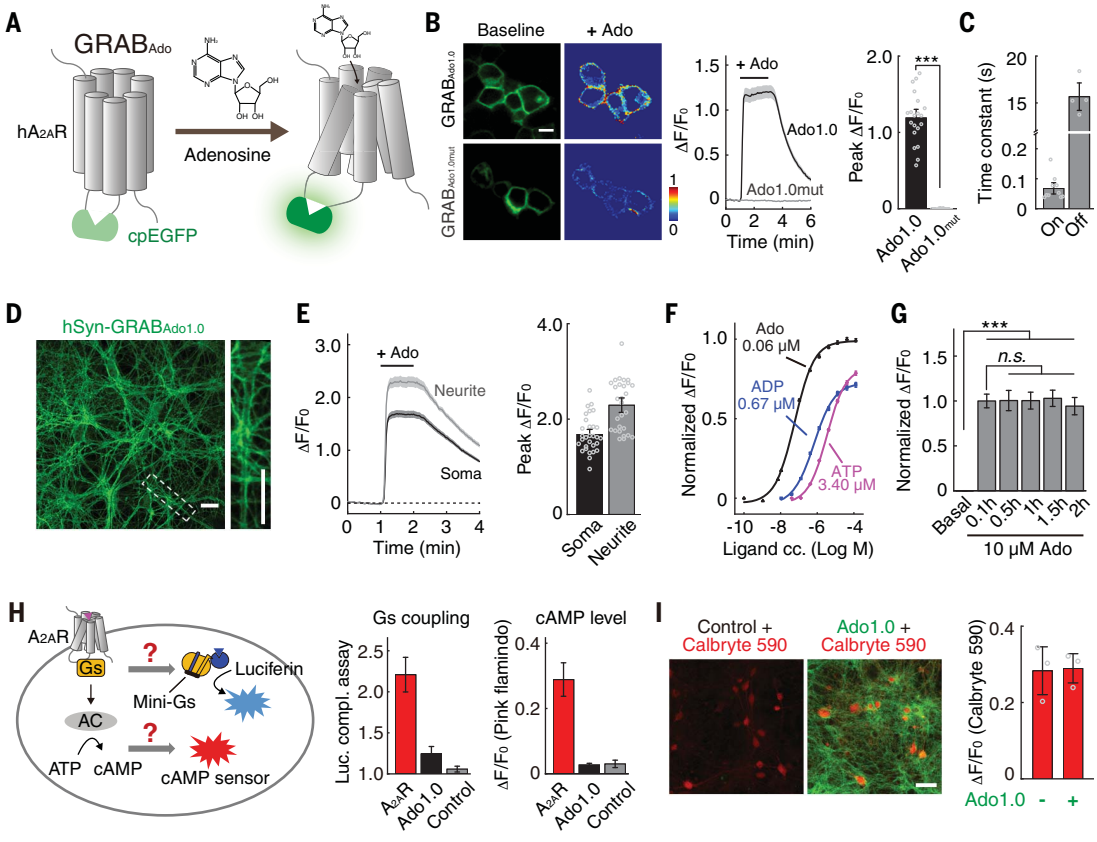


**Fig. 1. Design and characterization of genetically encoded adenosine sensors.** (**A**) Schematic drawing depicting the principle of the $GRAB_{Ado}$ sensors. The third intracellular loop of the human $A_{2A}R$ was replaced with cpEGFP; thus, the binding of adenosine induces a conformational change that increases the cpEGFP fluorescence. (**B**) Expression and responses of the $GRAB_{Ado1.0}$ and $GRAB_{Ado1.0mut}$ in HEK293T cells. (Left) Images of sensor fluorescence before and after application of 100 μM Ado (scale, 10 μm). (Middle and right) Time course and summary of peak $\Delta F/F_0$; $n$ = 20 cells from two cultures. (**C**) Rise and decay time constants of the Ado1.0 fluorescence in response to the application of Ado (100 μM) followed by the $A_{2A}R$ antagonist SCH-58261 (200 μM). $n$ = 10 and 4 cells, respectively. (**D**) Expression of Ado1.0 in cultured neurons (scale bars, 30 μm). (**E**) Response of Ado1.0 in cultured neurons; $n$ = 28 to 30 regions of interest (ROIs) in three cultures. (**F**) Normalized dose-response curves for Ado1.0-expressing neurons in response to Ado, ADP, and ATP; $n \geq 20$ ROIs each. (**G**) Normalized $\Delta F/F_0$ of Ado1.0-expressing neurons in response to 10 μM Ado applied for 2 hours; $n$ = 28 neurons from three cultures. (**H**) Ado1.0 does not engage downstream $G_s$ protein signaling. A luciferase complementation assay was used to measure $G_s$ protein coupling, and the cAMP sensor PinkFlamindo was used to measure cAMP concentrations in HEK293T or HeLa cells expressing $A_{2A}R$ or Ado1.0; $n \geq 3$ independent experiments each. (**I**) Expression of Ado1.0 has minimal effects on neuronal physiology. Calbryte 590 was used to measure $Ca^{2+}$ concentrations in Ado1.0-expressing neurons and control neurons. Confocal images (left; scale bar, 50 μm) and $\Delta F/F_0$ of Calbryte 590 in response to field stimuli (30 Hz, 100 pulses) (right); $n$ = 3 coverslips each.

nonbinding mutant form of the adenosine sensor (fig. S6 and Fig. 2D; Wake versus NREM: $P$ = 0.08; REM versus NREM: $P$ = 0.94). Benefiting from the high temporal resolution of the $GRAB_{Ado}$ sensor, we also observed a significantly higher amount of adenosine during REM sleep than during both wakefulness and NREM sleep (Fig. 2, B, C and E; REM versus Wake: $P$ = 0.002; REM versus NREM: $P = 1.7 \times 10^{-5}$). Such an increase during REM sleep could not be measured using microdialysis because of the short duration of REM sleep in mice (*9*, *23*). Furthermore, our measurements showed rapid change in the adenosine level as mice transitioned between three different brain states (Fig. 2, B and F), revealing an average rise time of 29.3 ± 3.6 s (mean ± SEM). This rapid change in extracellular adenosine levels suggests a neural activity–dependent release (*24*, *25*).

### Neural control of fast adenosine transients in the BF during the sleep-wake cycle

Next, we examined how the activity of different neuronal types in the BF contributes to the observed adenosine dynamics during the sleep-wake cycle. The BF neural circuits for the sleep-wake regulation have been characterized (*7*, *8*, *26*): Cholinergic neurons (expressing *choline acetyltransferase*, *ChAT*) and glutamatergic neurons (expressing *vesicular glutamate transporter 2*, *VGLUT2*) are highly active during both wakefulness and REM sleep, and optogenetic activation of these two cell types promotes wakefulness (*14*). We first examined the role of BF ChAT+ neurons by measuring the correlation between the activity of ChAT+ neurons and the change in extracellular adenosine concentration. We injected AAV expressing $GRAB_{Ado}$ into the BF of one hemisphere and AAV expressing the Cre-dependent $Ca^{2+}$ indicator GCaMP6s (*27*) into the contralateral BF of the ChAT-Cre mice (*28*), and measured the fluorescence signal using fiber photometry 2 weeks after injection (Fig. 3A and fig. S7). This "bilateral dual probes" method allowed us to simultaneously measure the signals of two interfering fluorescent probes in the same brain region. The population $Ca^{2+}$ activity of ChAT+ neurons had a time course similar to that of the extracellular adenosine increase (Fig. 3B). The size of $GRAB_{Ado}$ event strongly correlated with the size of the corresponding GCaMP event (Fig. 3C; Pearson's $r$ = 0.83, $P < 0.0001$), and such correlation was not observed when the GCaMP signals were randomly shuffled (Fig. 3D; Pearson's $r$ = 0.06, $P$ = 0.32). Moreover, the change in population $Ca^{2+}$ activity measured in ChAT+ neurons often preceded the change in the adenosine signal by ~24 s (Fig. 3E), suggesting that BF ChAT+ neurons may control the amount of extracellular adenosine (*29*, *30*).

We therefore optogenetically activated ChAT+ neurons and used fiber photometry to measure the evoked adenosine release by coinjecting AAVs expressing $GRAB_{Ado}$ and Cre-dependent red-shifted channelrhodopsin, ChrimsonR (*31*), into the BF of ChAT-Cre mice (Fig. 3F and fig. S8). Activating ChAT+ neurons (638 nm laser, 10 ms/pulse, 10 Hz for 8 s) induced a slight but significant increase in extracellular adenosine (Fig. 3, G to I; peak signal: $P$ = 0.014; $\Sigma_{Fluo.}$: $P$ = 0.023), indicating that ChAT+ neurons may indeed provide some contribution to the

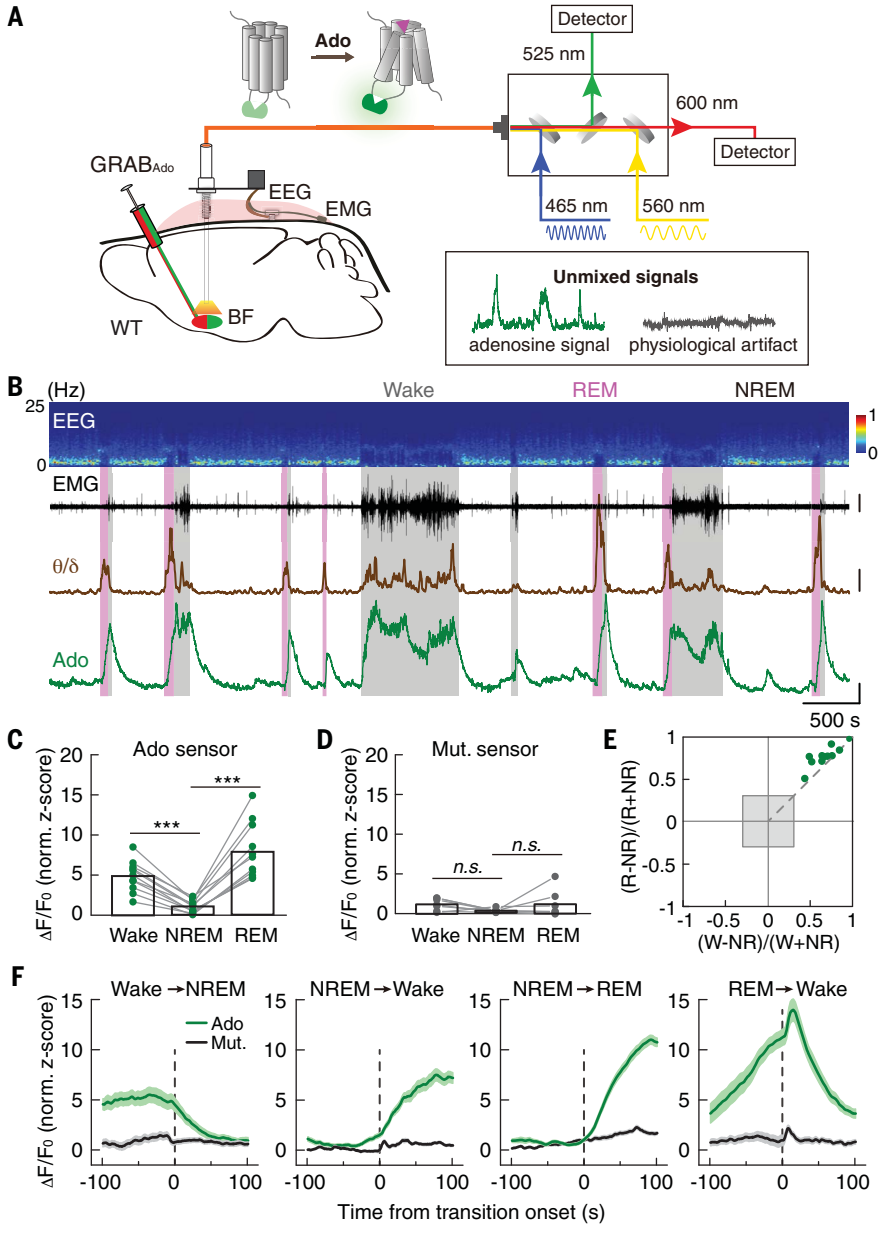


**Fig. 2. Adenosine dynamics in the mouse basal forebrain during the sleep-wake cycle.** (**A**) Schematic diagram depicting fiber photometry recording of extracellular adenosine during the sleep-wake cycle in freely moving mice. (**B**) (Top to bottom) EEG power spectrogram; electromyogram (EMG) (scale, 0.5 mV); ratio between EEG theta power (θ) and delta power (δ) (scale, 2); $GRAB_{Ado}$ fluorescence (scale, 1 *z*-score). The brain states (fig. S5) are color-coded; the same color code is used in all the following figures. (**C**) $GRAB_{Ado}$ fluorescence in different brain states. Each line represents data from one recording. $n = 11$ sessions from four mice. ***$P < 0.001$ (Student's paired $t$ test); Wake versus NREM: $P = 3.6 \times 10^{-6}$; REM versus NREM: $P = 1.7 \times 10^{-5}$. In this and all subsequent figures, summary data are expressed as the mean ± SEM. (**D**) Fluorescence of the mutant sensor in different brain states. $n = 7$ sessions from four mice. n.s., not significant (Wilcoxon signed-rank test); Wake versus NREM: $P = 0.08$; REM versus NREM: $P = 0.94$. (**E**) Normalized modulation of $GRAB_{Ado}$ signal in REM (R) − NREM (NR) versus Wake (W) − NREM. Each symbol represents one recording, and the gray shaded box indicates a <2-fold signal change between the indicated brain states. (**F**) Signal of the $GRAB_{Ado}$ sensor and mutant sensor during brain state transitions. The vertical dashed lines represent the transition time. $n = 35$, 104, 148, and 29 events (in four mice) for each panel, respectively.

observed changes in extracellular adenosine during the sleep-wake cycle. However, the amplitude of evoked adenosine changes was highly variable in different trials (Fig. 3G), suggesting that other cell types in the BF may also play a role in regulating extracellular adenosine during the sleep-wake cycle.

We thus further examined the role of BF VGLUT2+ neurons, using the same "bilateral dual probes" method described above for expressing $GRAB_{Ado}$ and GCaMP6s in the BF of VGLUT2-Cre mice (*32*) (Fig. 4A and fig. S9). The $Ca^{2+}$ signal measured in VGLUT2+ neurons was significantly correlated with extracellular adenosine (Fig. 4, B to D; Pearson's $r = 0.64$, $P < 0.0001$) and preceded the $GRAB_{Ado}$ signal by ~41 s (Fig. 4E). Further optogenetic activation of VGLUT2+ neurons (Fig. 4F and fig. S10) at a physiologically relevant frequency of 20 Hz for 8 s (*14*) induced a large and reproducible increase in extracellular adenosine (Fig. 4, G to I; signal peak: $P = 0.036$; $\Sigma_{Fluo.}$: $P = 8 \times 10^{-5}$). This release was much larger than that induced by activating ChAT+ neurons (Fig. 4I; ChAT+ versus VGLUT2+, signal peak (*z*-score): 0.76 ± 0.20 versus 2.56 ± 0.21, $P = 0.0022$; $\Sigma_{Fluo.}$(*z*-score): 73 ± 22 versus 208 ± 17, $P = 0.0011$). The laser-induced increase in extracellular adenosine was likely due to direct activation of VGLUT2+ and ChAT+ neurons rather than nonspecific effects of the laser (e.g., local heating), because no significant laser-evoked fluorescence was observed in mice expressing only $GRAB_{Ado}$ but without ChrimsonR (fig. S11; $P = 0.45$). The difference that we observed between adenosine release evoked by the activation of ChAT+ or VGLUT2+ neurons most likely reflects their in vivo ability to control the adenosine dynamics during the sleep-wake cycle, because we used physiological firing rates for optogenetic activation of ChAT+ and VGLUT2+ neurons (10 and 20 Hz, respectively) (*14*, *33*).

We next measured the adenosine transients after selectively ablating VGLUT2+ neurons in the BF using Caspase-3 to drive cell type–specific apoptosis (*34*). We coinjected AAVs expressing $GRAB_{Ado}$ and Cre-dependent Caspase-3 in the BF of VGLUT2-Cre mice (Fig. 4J). Two weeks after injection, when a significant reduction in the number of VGLUT2+ neurons was observed in the BF (fig. S12), we found a significantly reduced extracellular adenosine increase during both wakefulness and REM

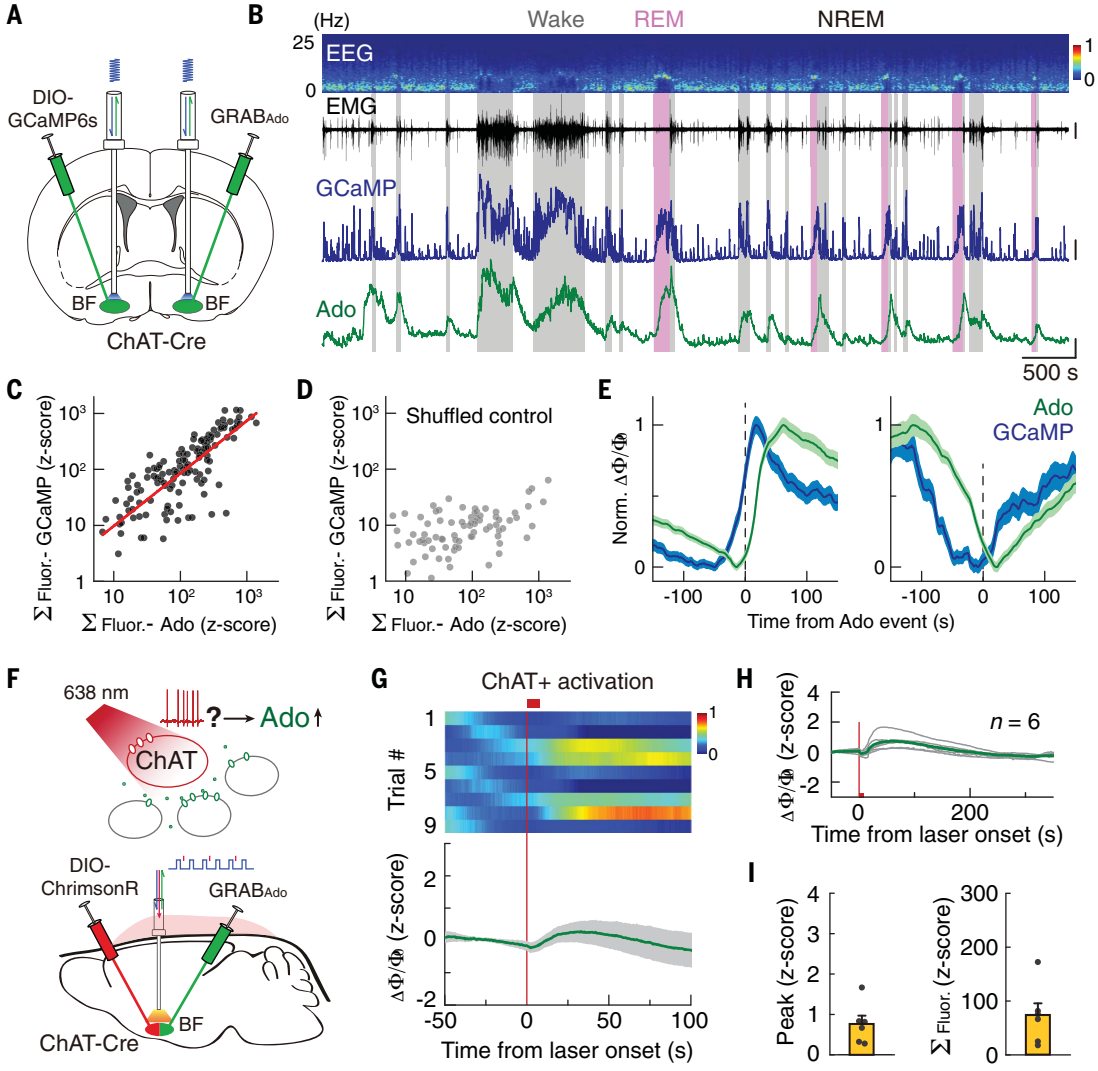


**Fig. 3. Calcium activity in BF cholinergic neurons correlates with changes in extracellular adenosine.** (**A**) Schematic diagram depicting fiber photometry recording of extracellular adenosine levels and population $Ca^{2+}$ activity of ChAT+ neurons. (**B**) (Top to bottom) EEG power spectrogram, EMG (scale, 0.1 mV), GCaMP fluorescence (scale, 1 *z*-score), and $GRAB_{Ado}$ fluorescence (scale, 1 *z*-score). (**C**) Correlation between the size of GCaMP and $GRAB_{Ado}$ events. The red line represents a linear fit. $n = 224$ events from nine recordings in three mice. Pearson's $r = 0.83$, $P < 0.0001$. The correlation coefficient was calculated using raw data (rather than using data after log transformation); the scatter plot is on a $\log_{10}$ scale for better visualization; thus, data points near zero may not be visible; the same analysis was applied in Fig. 3D and Fig. 4, C and D. (**D**) Same as in (C) after the GCaMP signal was randomly shuffled. Pearson's $r = 0.06$, $P = 0.32$. (**E**) Time course of the GCaMP and $GRAB_{Ado}$ signal aligned to the onset (left) or offset (right) of the $GRAB_{Ado}$ events. (**F**) Schematic diagram depicting fiber photometry recording of extracellular adenosine levels induced by optogenetic activation of ChAT+ neurons. (**G**) $GRAB_{Ado}$ signals evoked by optogenetic activation of ChAT+ neurons (638 nm laser, 10 ms/pulse, 10 Hz for 8 s). (Upper panel) Heat map plot of nine successive trials; (lower panel) averaged signal; red line, start of the laser train. (**H**) Group summary of laser-evoked $GRAB_{Ado}$ signals. Gray, data of individual recording; green, group average. (**I**) Quantification of laser-evoked adenosine signals in (H). (Left) Peak amplitude ($P = 0.014$, Student's *t* test); (right) integrated signal area ($P = 0.023$, Student's *t* test.).

sleep, as compared to control mice (Fig. 4, K and L; VGLUT2 lesion versus no-lesion, Wake (normalized $\Delta F/F_0$, norm. *z*-score): 1.6 ± 0.7 versus 5.3 ± 0.6, $P = 0.002$; NREM: 0.4 ± 0.2 versus 1.0 ± 0.1, $P = 0.017$; REM: 1.4 ± 1.0 versus 7.1 ± 0.8, $P = 0.0003$), further supporting the role of BF VGLUT2+ neurons in controlling the increase in extracellular adenosine.

### Loss of BF glutamatergic neurons impairs sleep homeostasis

The increase in adenosine during physiological or prolonged wakefulness has been suggested to powerfully control sleep homeostasis (*9*, *11*, *12*). Animals with lower activation of adenosine signaling may have a slower buildup of sleep pressure and exert increased wakefulness and faster recovery from prolonged wakefulness (*35*, *36*). Loss of VGLUT2+ neurons in the BF (e.g., through selective ablation) might thus alter sleep homeostasis.

To test this hypothesis, we bilaterally ablated VGLUT2+ neurons in the BF using the same method as described above and measured changes in the sleep-wake behavior (Fig. 5A). Mice with ablated BF VGLUT2+ neurons spent significantly more time in wakefulness compared to littermate controls (Fig. 5, B and C, and fig. S13; Lesion versus Control, time in wakefulness (%): 66.8 ± 1.5 versus 57.5 ± 2.6, $P = 0.0092$). This difference was primarily due to increased wakefulness specifically during the active period (i.e., nighttime), with no significant difference during the inactive period (i.e., daytime) (Fig. 5C; Lesion versus Control, time in wakefulness (%): nighttime, 91.3 ± 1.6 versus 76.3 ± 5.0, $P = 0.0041$; daytime, 42.2 ± 2.2 versus 38.6 ± 0.97, $P = 0.16$). We observed no apparent difference in the quality of the sleep or wakefulness in the lesion group, as measured by the power of electroencephalogram (EEG) slow-wave activity (SWA, 0.5 to 4 Hz) during NREM sleep or theta activity (6 to 10 Hz) during active wakefulness (*37*) (fig. S14; EEG SWA, $P = 0.87$; EEG theta, $P = 0.44$), suggesting that the observed increase in wakefulness in the lesion group was not caused by distorted patterns of brain oscillations.

Another measurement of impaired sleep homeostasis regulation is the change in recovery sleep after prolonged wakefulness (*1*, *38*). We thus examined whether the loss of VGLUT2+ neurons in the BF affects recovery sleep. Mice were kept in wakefulness by gentle handling (i.e., sleep deprivation, SD) in their home cages for 6 hours starting from the beginning of the light-on period, and recovery sleep was then

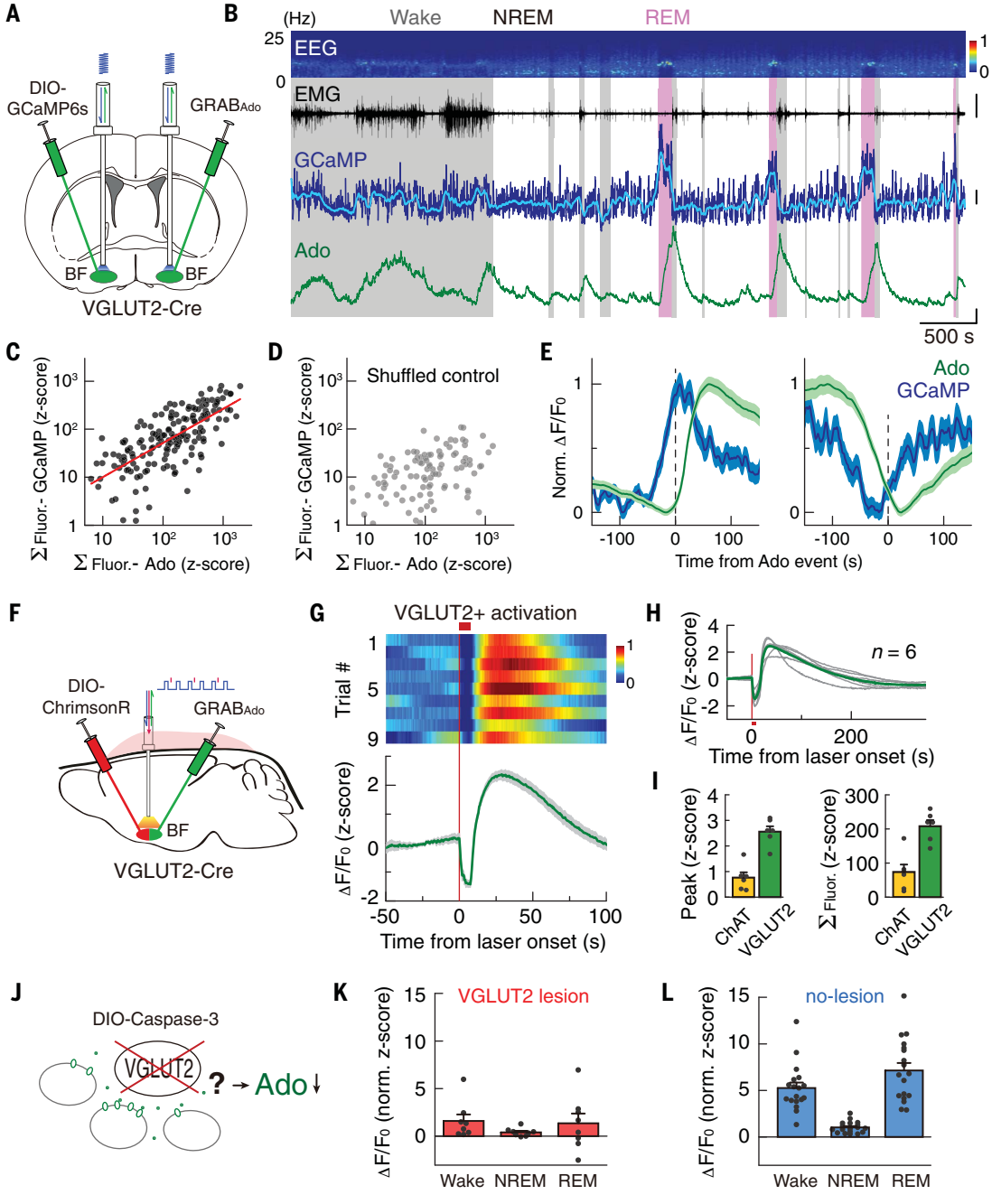


**Fig. 4. Glutamatergic neurons in the BF contribute to the increase in extracellular adenosine during the sleep-wake cycle.** (**A**) Schematic diagram depicting fiber photometry recording of extracellular adenosine levels and population $Ca^{2+}$ activity of VGLUT2+ neurons. (**B**) (Top to bottom) EEG power spectrogram, EMG (scale, 0.2 mV), GCaMP fluorescence (scale, 1 *z*-score; light blue, smoothed signal), and $GRAB_{Ado}$ fluorescence (scale, 1 *z*-score). (**C** and **D**) Same as Fig. 3, C and D, respectively. $n$ = 233 events from 10 recordings in six mice. In (C), Pearson's $r$ = 0.64, $P < 0.0001$; in (D), Pearson's $r$ = −0.07, $P$ = 0.3. (**E**) Same as Fig. 3E. (**F** to **H**) Same as Fig. 3, F to H, respectively, except that VGLUT2+ neurons are stimulated. The decrease in $GRAB_{Ado}$ signal after the laser onset was independent of extracellular adenosine because it cannot be blocked by an antagonist of the $GRAB_{Ado}$ sensor (*45*) and may be caused by activity-dependent PMCA effect (*46*). (**I**) Quantification of laser-evoked adenosine signals. Data of the ChAT+ group are the same as those in Fig. 3I. (Left) $P < 0.005$ (Wilcoxon rank-sum test); (right) $P < 0.002$ (Student's $t$ test). (**J**) Schematic diagram depicting the strategy used to selectively ablate VGLUT2+ neurons in the BF using a Cre-dependent Caspase-3. (**K** and **L**) Summary of $GRAB_{Ado}$ signal in mice with ablation of VGLUT2+ neurons (K) ($n$ = 8 recordings from eight mice) and in control mice (L) ($n$ = 18 recordings from 18 mice). Lesion versus Control: Wake, $P$ = 0.002 (Wilcoxon rank-sum test); NREM: $P$ = 0.017 (Student's $t$ test); REM: $P$ = 0.0003 (Student's $t$ test).

measured during the subsequent 18 hours (Fig. 5D and fig. S15) (*39*). Although both lesion and control mice showed compensatory sleep rebound (fig. S16), there was significantly less NREM sleep in the lesion group during ZT 12–16 (Fig. 5, D and E; Lesion versus Control, time in NREM (%): 12.9 ± 4.0 versus 35.2 ± 3.9, $P$ = 0.0017), but not for ZT 6–12 (Fig. 5D and E; $P$ = 0.90). We also analyzed the time course of the NREM SWA and NREM percentage after SD by fitting the hourly data with an exponential decay function (*38*). The lesion group exhibited a tendency of faster decline in the NREM SWA (fig. S17; decline coefficients: Lesion, −0.061 ± 0.011; Control, −0.033 ± 0.012; $P$ = 0.11) and a significantly faster decline in the NREM sleep time (Fig. 5F and G; decline coefficients: Lesion, −0.18 ± 0.011; Control, −0.094 ± 0.014; $P = 2.7 \times 10^{-4}$).

## Discussion

Here, we reported the design and characterization of a genetically encoded adenosine sensor ($GRAB_{Ado}$) with high sensitivity and specificity, and high temporal resolution; by combining the $GRAB_{Ado}$ and fiber photometry imaging with bilateral dual probes, together with optogenetic manipulation and cell type–specific lesion, we demonstrated a neuronal type–specific control of fast adenosine dynamics during the sleep-wake cycle and uncovered a critical role of the VGLUT2+ neurons in the BF in controlling adenosine dynamics and sleep homeostasis.

The cell type–specific control of extracellular adenosine levels in the BF suggests a distinct

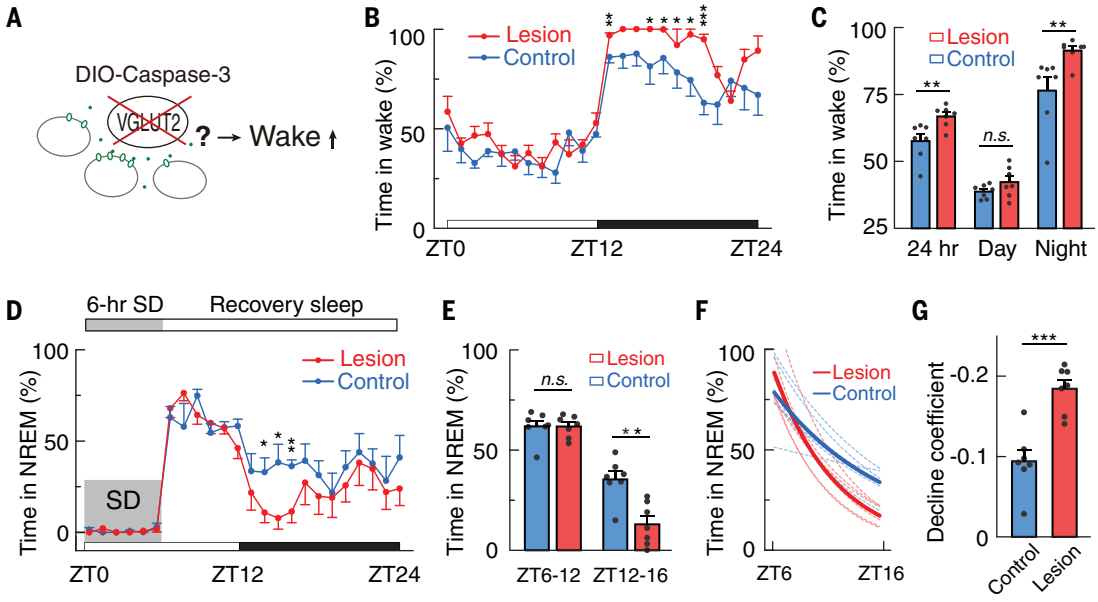


**Fig. 5. Loss of BF VGLUT2+ neurons impairs sleep homeostasis.** (**A**) Schematic diagram depicting the strategy used to selectively ablate VGLUT2+ neurons in the BF. (**B**) Circadian variation of wakefulness in lesion and control mice. $n = 7$ mice per group. $^{*}P < 0.05$, $^{**}P < 0.01$, and $^{***}P < 0.001$ (Wilcoxon rank-sum test or Student's $t$ test). (**C**) Percentage of time in wakefulness in the entire 24 hours, during the day or the night. $^{**}P < 0.01$; n.s., not significant; 24-hr, $P = 0.0092$ (Student's $t$ test); Day, $P = 0.16$ (Student's $t$-test); Night, $P = 0.0041$ (Wilcoxon rank-sum test). (**D**) Circadian variation of the NREM sleep when the lesion and control mice were subjected to sleep deprivation (SD) for 6 hours (ZT0-6). $n = 7$ mice per group. $^{*}P < 0.05$ and $^{**}P < 0.01$ (Wilcoxon rank-sum test or Student's $t$ test). (**E**) Summary of the percentage of NREM sleep during the two selected periods. $^{**}P < 0.01$ and n.s., not significant. ZT6-12, $P = 0.90$ (Wilcoxon rank-sum test); ZT12-16, $P = 0.0017$, (Student's $t$ test). (**F**) Time course showing the decay in the percentage of NREM sleep in each hour after SD using the same data in (D). Dashed lines, the exponential fit of data from individual mice; solid line, group average. (**G**) Fitting coefficients from the data in (F) (smaller coefficient means a faster decline in hourly sleep percentage). $P = 2.7 \times 10^{-4}$ (Student's $t$ test).

contribution to the sleep-wake regulation by different wake-active neurons in the BF. The long delay in the increase of extracellular adenosine following neural activation may provide a time window for the activation of BF neural circuits, while still maintaining a feedback inhibition (*40*) for stabilizing the network.

Our results that the loss of BF VGLUT2+ neurons have a larger effect on the balance between the duration of sleep and wakefulness, but not the SWA or the recovery sleep, are consistent with the notion that adenosine regulation of SWA is primarily caused by its direct modulation of neural activity in the thalamocortical system (*12*, *41*, *42*). This result suggests a dissociation in the regulation of different features of the sleep-wake cycle.

Together, our findings offer new insights into the mechanisms by which neural activity during wakefulness contributes to the increase in sleep pressure (*43*, *44*) by stimulating the release of somnogenic factors.

## Materials and Methods

### *Design and characterization of GRAB$_{Ado}$*

The cDNAs encoding various subtypes of Ado receptor were amplified from the human GPCR cDNA library, and the third intracellular loop (ICL3) of each receptor was replaced with the ICL3 of GRAB$_{NE}$. The insertion sites on $A_{2A}R$ and the amino acid composition between $A_{2A}R$ and ICL3 of GRAB$_{NE}$ were systematically screened to obtain GRAB$_{Ado1.0}$. GRAB$_{Ado1.0}$ was then expressed in HEK293T cells, HeLa cells, or cultured rat primary neurons for further characterization of its sensitivity and specificity, its coupling with intracellular signaling pathways, and effects of its expression on neuronal physiology.

### *Animals and surgical procedures*

All animal experimental procedures followed guidelines of the National Institutes of Health and were approved by the Animal Care and Use Committee at Peking University, or the Institute of Neuroscience, Chinese Academy of Sciences. Both male and female mice (>7 weeks at the time of surgery) were used for in vivo experiments. AAV virus (0.2 to 0.4 μl) was stereotaxically injected into the BF using a glass pipette micro-injector through a craniotomy. For fiber photometry and optogenetic activation experiments, optical fibers were inserted into the BF using the same coordinate for virus injections. EEG and EMG electrodes were attached according to standard procedures. All implants were secured using dental cement. Experiments were carried out at least 1 week after surgery.

### *Polysomnography recordings*

The EEG and EMG signals were recorded using TDT amplifiers with a high-pass filter at 0.5 Hz and digitized at 1500 Hz. The brain states were scored every 5 s semi-automatically in MATLAB using fast Fourier transform (FFT) spectral analysis with a frequency resolution of 0.18 Hz, and the results were validated manually by trained experimenters according to established criteria. For recording with fiber photometry, experiments were carried out in home cages, and each session lasted ~3 hours. For long-term recording, mice were connected to the system using a commutator and habituated for at least 3 days before a 3-day recording period, followed by 6-hour sleep deprivation and recovery sleep for 30 hours. Sleep deprivation was achieved using gentle handling methods.

### *Fiber photometry recording and analysis*

GRAB$_{Ado}$ and GCaMP fluorescence was recorded using fiber photometry with lock-in detection. The fiber photometry rig was built using parts from Doric Lens, and the lock-in detection was implemented in the TDT RZ2 system using the fiber photometry "Gizmo" of the Synapse software. The demodulated signal was low-pass filtered at 20 Hz and stored using a sampling frequency of 1017 Hz. To analyze the photometry data, we first down-sampled the raw data to 1 Hz and subtracted the background autofluorescence. We then calculated the $\Delta F/F_0$ using a baseline obtained by fitting the autofluorescence-subtracted data with a second-order exponential function. Finally, we used a MATLAB script "BEADS" with a cut-off frequency of 0.00035 cycles per sample to remove the slow drift and identify fast components. To quantify the GRAB$_{Ado}$ signal across different animals, the z-score transformed $\Delta F/F_0$ was further normalized using the standard deviation of the signal during NREM sleep.

### Statistics

A normality test was first performed on each dataset using the Shapiro-Wilk test. The parametric tests were used if the dataset was normally distributed; otherwise, nonparametric tests were used. All the statistical tests were two-tailed and performed in MATLAB. Data in the fiber photometry experiments were excluded based on post-hoc verification of the virus expression and the position of optical fibers. In the long-term polysomnographic recording experiments, one mouse was excluded for analysis because of abnormal EEG and EMG signals. The investigators were not blinded to the genotypes or the experimental conditions of the animals.

Further details of the materials and methods can be found in the supplementary materials.

## REFERENCES AND NOTES


1. A. A. Borbély, A two process model of sleep regulation. *Hum. Neurobiol.* **1**, 195–204 (1982). pmid: 7185792
2. A. A. Borbély, P. Achermann, Sleep homeostasis and models of sleep regulation. *J. Biol. Rhythms* **14**, 557–568 (1999). pmid: 10643753
3. R. Allada, C. Cirelli, A. Sehgal, Molecular Mechanisms of Sleep Homeostasis in Flies and Mammals. *Cold Spring Harb. Perspect. Biol.* **9**, a027730 (2017). doi: 10.1101/cshperspect.a027730; pmid: 28432135
4. Z. Wang *et al*., Quantitative phosphoproteomic analysis of the molecular substrates of sleep need. *Nature* **558**, 435–439 (2018). doi: 10.1038/s41586-018-0218-8; pmid: 29899451
5. A. Kempf, S. M. Song, C. B. Talbot, G. Miesenböck, A potassium channel β-subunit couples mitochondrial electron transport to sleep. *Nature* **568**, 230–234 (2019). doi: 10.1038/s41586-019-1034-5; pmid: 30894743
6. V. V. Vyazovskiy *et al*., Cortical firing and sleep homeostasis. *Neuron* **63**, 865–878 (2009). doi: 10.1016/j.neuron.2009.08.024; pmid: 19778514
7. R. E. Brown, R. Basheer, J. T. McKenna, R. E. Strecker, R. W. McCarley, Control of sleep and wakefulness. *Physiol. Rev.* **92**, 1087–1187 (2012). doi: 10.1152/physrev.00032.2011; pmid: 22811426
8. T. E. Scammell, E. Arrigoni, J. O. Lipton, Neural Circuitry of Wakefulness and Sleep. *Neuron* **93**, 747–765 (2017). doi: 10.1016/j.neuron.2017.01.014; pmid: 28231463
9. T. Porkka-Heiskanen *et al*., Adenosine: A mediator of the sleep-inducing effects of prolonged wakefulness. *Science* **276**, 1265–1268 (1997). doi: 10.1126/science.276.5316.1265; pmid: 9157887
10. T. Porkka-Heiskanen, R. E. Strecker, R. W. McCarley, Brain site-specificity of extracellular adenosine concentration changes during sleep deprivation and spontaneous sleep: An in vivo microdialysis study. *Neuroscience* **99**, 507–517 (2000). doi: 10.1016/S0306-4522(00)00220-7; pmid: 11029542
11. R. Basheer, R. E. Strecker, M. M. Thakkar, R. W. McCarley, Adenosine and sleep-wake regulation. *Prog. Neurobiol.* **73**, 379–396 (2004). doi: 10.1016/j.pneurobio.2004.06.004; pmid: 15313333
12. R. W. Greene, T. E. Bjorness, A. Suzuki, The adenosine-mediated, neuronal-glial, homeostatic sleep response. *Curr. Opin. Neurobiol.* **44**, 236–242 (2017). doi: 10.1016/j.conb.2017.05.015; pmid: 28633050
13. C. Anaclet *et al*., Basal forebrain control of wakefulness and cortical rhythms. *Nat. Commun.* **6**, 8744 (2015). doi: 10.1038/ncomms9744; pmid: 26524973
14. M. Xu *et al*., Basal forebrain circuit for sleep-wake control. *Nat. Neurosci.* **18**, 1641–1647 (2015). doi: 10.1038/nn.4143; pmid: 26457552
15. M. Jing *et al*., A genetically encoded fluorescent acetylcholine indicator for in vitro and in vivo studies. *Nat. Biotechnol.* **36**, 726–737 (2018). doi: 10.1038/nbt.4184; pmid: 29985477
16. F. Sun *et al*., A Genetically Encoded Fluorescent Sensor Enables Rapid and Specific Detection of Dopamine in Flies, Fish, and Mice. *Cell* **174**, 481–496.e19 (2018). doi: 10.1016/j.cell.2018.06.042; pmid: 30007419
17. J. Feng *et al*., A Genetically Encoded Fluorescent Sensor for Rapid and Specific In Vivo Detection of Norepinephrine. *Neuron* **102**, 745–761.e8 (2019). doi: 10.1016/j.neuron.2019.02.037; pmid: 30922875
18. M. Jing *et al*., An optimized acetylcholine sensor for monitoring in vivo cholinergic activity. *bioRxiv* 861690 [Preprint]. (2 December 2019). https://doi.org/10.1101/861690.
19. F. Sun *et al*., New and improved GRAB fluorescent sensors for monitoring dopaminergic activity in vivo. *bioRxiv* 2020.03.28.013722 [Preprint]. (2020). https://doi.org/10.1101/2020.03.28.013722.
20. J. Wan *et al*., A genetically encoded GRAB sensor for measuring serotonin dynamics in vivo. *bioRxiv* 2020.02.24.962282 [Preprint] (2020). https://doi.org/10.1101/2020.02.24.962282.
21. G. Lebon *et al*., Agonist-bound adenosine A2A receptor structures reveal common features of GPCR activation. *Nature* **474**, 521–525 (2011). doi: 10.1038/nature10136; pmid: 21593763
22. J. D. Marshall *et al*., Cell-Type-Specific Optical Recording of Membrane Voltage Dynamics in Freely Moving Mice. *Cell* **167**, 1650–1662.e15 (2016). doi: 10.1016/j.cell.2016.11.021; pmid: 27912066
23. B. B. McShane *et al*., Characterization of the bout durations of sleep and wakefulness. *J. Neurosci. Methods* **193**, 321–333 (2010). doi: 10.1016/j.jneumeth.2010.08.024; pmid: 20817037
24. M. Wall, N. Dale, Activity-dependent release of adenosine: A critical re-evaluation of mechanism. *Curr. Neuropharmacol.* **6**, 329–337 (2008). doi: 10.2174/157015908787386087; pmid: 19587854
25. D. Lovatt *et al*., Neuronal adenosine release, and not astrocytic ATP release, mediates feedback inhibition of excitatory activity. *Proc. Natl. Acad. Sci. U.S.A.* **109**, 6265–6270 (2012). doi: 10.1073/pnas.1120997109; pmid: 22421436
26. F. Weber, Y. Dan, Circuit-based interrogation of sleep control. *Nature* **538**, 51–59 (2016). doi: 10.1038/nature19773; pmid: 27708309
27. T. W. Chen *et al*., Ultrasensitive fluorescent proteins for imaging neuronal activity. *Nature* **499**, 295–300 (2013). doi: 10.1038/nature12354; pmid: 23868258
28. J. Rossi *et al*., Melanocortin-4 receptors expressed by cholinergic neurons regulate energy balance and glucose homeostasis. *Cell Metab.* **13**, 195–204 (2011). doi: 10.1016/j.cmet.2011.01.010; pmid: 21284986
29. C. Blanco-Centurion *et al*., Adenosine and sleep homeostasis in the Basal forebrain. *J. Neurosci.* **26**, 8092–8100 (2006). doi: 10.1523/JNEUROSCI.2181-06.2006; pmid: 16885223
30. A. V. Kalinchuk, R. W. McCarley, D. Stenberg, T. Porkka-Heiskanen, R. Basheer, The role of cholinergic basal forebrain neurons in adenosine-mediated homeostatic control of sleep: Lessons from 192 IgG-saporin lesions. *Neuroscience* **157**, 238–253 (2008). doi: 10.1016/j.neuroscience.2008.08.040; pmid: 18805464
31. N. C. Klapoetke *et al*., Independent optical excitation of distinct neural populations. *Nat. Methods* **11**, 338–346 (2014). doi: 10.1038/nmeth.2836; pmid: 24509633
32. L. Vong *et al*., Leptin action on GABAergic neurons prevents obesity and reduces inhibitory tone to POMC neurons. *Neuron* **71**, 142–154 (2011). doi: 10.1016/j.neuron.2011.05.028; pmid: 21745644
33. M. G. Lee, O. K. Hassani, A. Alonso, B. E. Jones, Cholinergic basal forebrain neurons burst with theta during waking and paradoxical sleep. *J. Neurosci.* **25**, 4365–4369 (2005). doi: 10.1523/JNEUROSCI.0178-05.2005; pmid: 15858062
34. C. F. Yang *et al*., Sexually dimorphic neurons in the ventromedial hypothalamus govern mating in both sexes and aggression in males. *Cell* **153**, 896–909 (2013). doi: 10.1016/j.cell.2013.04.017; pmid: 23663785
35. S. Palchykova *et al*., Manipulation of adenosine kinase affects sleep regulation in mice. *J. Neurosci.* **30**, 13157–13165 (2010). doi: 10.1523/JNEUROSCI.1359-10.2010; pmid: 20881134
36. T. E. Bjorness *et al*., An Adenosine-Mediated Glial-Neuronal Circuit for Homeostatic Sleep. *J. Neurosci.* **36**, 3709–3721 (2016). doi: 10.1523/JNEUROSCI.3906-15.2016; pmid: 27030757
37. V. V. Vyazovskiy, I. Tobler, Theta activity in the waking EEG is a marker of sleep propensity in the rat. *Brain Res.* **1050**, 64–71 (2005). doi: 10.1016/j.brainres.2005.05.022; pmid: 15975563
38. P. Franken, I. Tobler, A. A. Borbély, Sleep homeostasis in the rat: Simulation of the time course of EEG slow-wave activity. *Neurosci. Lett.* **130**, 141–144 (1991). doi: 10.1016/0304-3940(91)90382-4; pmid: 1795873
39. P. Franken, A. Malafosse, M. Tafti, Genetic determinants of sleep regulation in inbred mice. *Sleep* **22**, 155–169 (1999). pmid: 10201060
40. R. W. Greene, H. L. Haas, The electrophysiology of adenosine in the mammalian central nervous system. *Prog. Neurobiol.* **36**, 329–341 (1991). doi: 10.1016/0301-0082(91)90005-L; pmid: 1678539
41. H. C. Heller, A global rather than local role for adenosine in sleep homeostasis. *Sleep* **29**, 1382–1383, discussion 1387–1389 (2006). doi: 10.1093/sleep/29.11.1382; pmid: 17162982
42. M. D. Noor Alam, R. Szymusiak, D. McGinty, Adenosinergic regulation of sleep: Multiple sites of action in the brain. *Sleep* **29**, 1384–1385, discussion 1387–1389 (2006). doi: 10.1093/sleep/29.11.1384; pmid: 17162983
43. M. Jouvet, Sleep and serotonin: An unfinished story. *Neuropsychopharmacology* **21** (suppl.), 24S–27S (1999). pmid: 10432485
44. G. Oikonomou *et al*., The Serotonergic Raphe Promote Sleep in Zebrafish and Mice. *Neuron* **103**, 686–701.e8 (2019). doi: 10.1016/j.neuron.2019.05.038; pmid: 31248729
45. Z. Wu *et al*., A GRAB sensor reveals activity-dependent non-vesicular somatodendritic adenosine release. *bioRxiv* 2020.05.04.075564 [Preprint]. (2020). doi: 10.1101/2020.05.04.075564
46. Z. Zhang, K. T. Nguyen, E. F. Barrett, G. David, Vesicular ATPase inserted into the plasma membrane of motor terminals by exocytosis alkalinizes cytosolic pH and facilitates endocytosis. *Neuron* **68**, 1097–1108 (2010). doi: 10.1016/j.neuron.2010.11.035; pmid: 21172612


## ACKNOWLEDGMENTS

We thank M. Poo and Z. Liang for critical reading of the manuscript; M. Yanagisawa, Y. Dan, E. Herzog, M. Luo, D. Prober, and A. Adamantidis for comments or suggestions; and H. Wang, H. Wu, Y. Wan, M. Jing, A. Dong, and S. Pan for assistance during in vitro sensor screening and characterization. **Funding:** This work was supported by the 'Strategic Priority Research Program' of the Chinese Academy of Sciences (XDB32010000 to M.X.), grants from NSFC (31871074 to M.X., 91832000 to Y.L., 31871051 to S.Z.), National Key R&D Program of China (2017YFE0196600 to M.X.), Shanghai Municipal Science and Technology Major Project (2018SHZDZX05 to M.X., 18JC1420302 to S.Z.), Beijing Municipal Science & Technology Commission (Z181100001318002 and Z181100001518004 to Y.L.), the Guangdong Grant 'Key Technologies for Treatment of Brain Disorders' (2018B030332001 to Y.L.), and Shanghai Pujiang Program (18PJ1410800 to M.X.). Z.W. is supported by the Boehringer Ingelheim–Peking University Postdoctoral Program. **Author contributions:** M.X. conceived and supervised the projects; Z.W. performed all experiments and data analysis on the design and verification of the $GRAB_{Ado}$ probe under the supervision of Y.L., and all other experiments and data analysis were performed by M.X., W.P., and K.S; M.X., W.P., K.S., S.Z., and Y.L. contributed to data interpretation. M.X., Y.L., and S.Z. wrote the manuscript with inputs from all other authors. **Competing interests:** Z.W. and Y.L. have filed patent applications of which the value might be affected by this publication. **Data and materials availability:** All data necessary to assess the conclusions of this manuscript are available in the manuscript or the supplementary materials. Constructs of the adenosine sensor have been deposited at Addgene and are available under a materials transfer agreement.

## SUPPLEMENTARY MATERIALS

science.sciencemag.org/content/369/6508/eabb0556/suppl/DC1
Materials and Methods
Figs. S1 to S17
References (*47*–*55*)
MDAR Reproducibility Checklist

View/request a protocol for this paper from *Bio-protocol*.

28 January 2020; resubmitted 19 May 2020
Accepted 3 July 2020
10.1126/science.abb0556

Science

# Regulation of sleep homeostasis mediator adenosine by basal forebrain glutamatergic neurons

Wanling Peng, Zhaofa Wu, Kun Song, Siyu Zhang, Yulong Li and Min Xu

*Science* **369** (6508), eabb0556.
DOI: 10.1126/science.abb0556

**Sleep and basal forebrain activity**

Different patterns of neural activity in the brain control the sleep-wake cycle. However, how this activity contributes to sleep homeostasis remains largely unknown. Adenosine in the basal forebrain is a prominent physiological mediator of sleep homeostasis. Using a newly developed indicator, Peng *et al.* monitored adenosine concentration in the mouse basal forebrain. There was a clear correlation with wake state and REM sleep. Activity-dependent release of adenosine could also be elicited after optogenetic stimulation of basal forebrain glutamatergic, but not cholinergic, neurons. These findings offer new insights into how neuronal activity during wakefulness contributes to sleep pressure through the release of sleep-inducing factors.

*Science*, this issue p. eabb0556